J. Phys. Chem. A 2008, 112, 744−751

Microhydration of X_2 Gas (X = Cl, Br, and I): A Theoretical Study on $X_2 \cdot nH_2O$ Clusters (n = 1−8)

A. K. Pathak,[†] **T. Mukherjee,**[†] **and D. K. Maity***[,‡]

Radiation and Photochemistry Division, and Theoretical Chemistry Section, Chemistry Group, Bhabha Atomic Research Centre, Mumbai 400085, India

Received: August 16, 2007; In Final Form: October 25, 2007

Structure and properties of hydrated clusters of halogen gas, $X_2 \cdot nH_2O$ (X = Cl, Br, and I; n = 1−8) are presented following first principle based electronic structure theory, namely, BHHLYP density functional and second-order Moller−Plesset perturbation (MP2) methods. Several geometrical arrangements are considered as initial guess structures to look for the minimum energy equilibrium structures by applying the 6-311++G(d,p) set of the basis function. Results on X_2−water clusters (X = Br and I) suggest that X_2 exists as a charge separated ion pair, $X^{+\delta}-X^{-\delta}$ in the hydrated clusters, $X_2 \cdot nH_2O$ ($n \geq 2$). Though the optimized structures of $Cl_2 \cdot nH_2O$ clusters look like $X_2 \cdot nH_2O$ (X = Br and I) clusters, Cl_2 does not exist as a charge separated ion pair in the presence of solvent water molecules. The calculated interaction energy between X_2 and solvent water cluster increases from $Cl_2 \cdot nH_2O$ to $I_2 \cdot nH_2O$ clusters, suggesting solubility of gas-phase I_2 in water to be a maximum among these three systems. Static and dynamic polarizabilities of hydrated X_2 clusters, $X_2 \cdot nH_2O$, are calculated and observed to vary linearly with the size (n) of these water clusters with correlation coefficient >0.999. This suggests that the polarizability of the larger size hydrated clusters can be reliably predicted. Static and dynamic polarizabilities of these hydrated clusters grow exponentially with the frequency of an external applied field for a particular size (n) of hydrated cluster.

1. Introduction

In recent years, the study on microhydration of neutral and charged chemical species has been a subject of intense research from both experimental and theoretical points of view. This is mainly because of the strong dependency of the properties on the size and geometry of the hydrated clusters of these species. When a solute is introduced to a solvent water medium, the water molecules in immediate proximity of the solute are rearranged to allow the solute to go through the solvation process. The electron distribution pattern of the added solute plays the key role of shaping up the structure of the water network around the solute. A plethora of experiment, theory, and simulation studies have been carried out to understand the structure and dynamics of microhydration on small negatively charged ions for their unique spectroscopic and thermodynamic properties.[1−16] The properties of these solute embedded water clusters provide a basic understanding of the fundamental interactions those are responsible for hydration process at the molecular level and thus it is important not only to chemists but also to physicists, biologists, and material scientists. It is also known that bromine gas is much more soluble than chlorine gas in water. But to the best of our knowledge no information is available on the solubility of iodine in gas phase. As these species have zero dipole moment, one has to apply explicit solvation model to study the solvent effect rather than taking a continuum model like Onsager's reaction field model. However, very little effort has been put to study microhydration of X_2 (X = Cl and Br) systems.[16−19] The molecular interaction between a neutral solute and solvent water molecules as well as the hydrogen bonding interactions among the solvent water molecules can be examined in such studies. Such studies will also provide information on the evolution of hydration motifs of X_2 systems in water. An important electronic effect in these hydrated clusters expected is the electronic polarizability, which is an important property to understand the process of solvation.[20−21] Electronic polarization in the condensed phase has guided to evolve polarizable point charge model in studying various properties and processes including solvent effect. Thus, a systematic study in halogen−water clusters will be of considerable interest. This will be very useful to understand solute−solvent and solvent−solvent intermolecular interactions in water medium and hence for molecular modeling in aqueous phase.[22] At present, various possible minimum energy configurations of $X_2 \cdot nH_2O$ cluster (X = Cl, Br and I; n = 1−8), bonding characteristics, energy parameters, and polarizability (both static and dynamic) are reported following first principle based electronic structure theory.

2. Theoretical Methods

To decide a suitable level of theoretical method for calculations, geometrical parameters and polarizability of mono- and dihydrated clusters of Cl_2 and Br_2 are carried out following correlated hybrid density functionals (B3LYP and BHHLYP) and second-order Moller−Plesset perturbation theory adopting triple split Gaussian type basis functions. It is observed that Becke's half-and-half (BHH) nonlocal exchange and Lee−Yang−Parr (LYP) nonlocal correlation functionals (BHHLYP) perform well to describe these clusters producing geometrical parameters and polarizabilities close to MP2 values. BHHLYP functional includes 50% Hartree−Fock exchange, 50% Slater exchange and the additional correlation effects of the LYP functional.[23] Geometry optimization on all the hydrated clusters

---

* Corresponding author. E-mail: dkmaity@barc.gov.in.

[†] Radiation and Photochemistry Division.

[‡] Theoretical Chemistry Section.

10.1021/jp076594a CCC: $40.75

has been carried out at BHHLYP level of theory to locate minimum energy structures followed by single point energy calculation at second-order Moller−Plesset perturbation theory (MP2) for improvement of energy by considering the electron correlation energy in a better way. Triple split valence basis function due to Pople including polarized and diffuse functions has been adopted for all calculations. The Newton−Raphson based algorithm has been applied to carry out geometry optimization for each of these molecular clusters with various initial guess structures to find out the most stable configuration without any symmetry restriction. Hessian calculations are also performed for all the equilibrium minimum energy structures to check the nature of predicted equilibrium geometry. Static response properties of a molecular system may be expressed by expanding the field-dependent energy $E(\mathbf{F})$ as a series of components of a uniform electric field $\mathbf{F}$,

$$E(\mathbf{F}) = E(0) + \sum_i \mu_i \mathbf{F}_i + \left(\frac{1}{2}\right)\sum_{ij} \alpha_{ij}\mathbf{F}_i\mathbf{F}_j + ...$$

where $E(0)$ is the energy of the system in absence of any electric field, μ is the dipole moment and α is the dipole polarizability tensor. The polarizability of these hydrated molecular clusters is calculated from the diagonal elements of the polarizability tensor,

$$\alpha = \frac{1}{3}(\alpha_{xx} + \alpha_{yy} + \alpha_{zz})$$

The components of the polarizability tensor are the second-order derivatives of energy with respect to the Cartesian components (i, $j = x, y, z$) of the applied electric field ($\mathbf{F}$),

$$\alpha_{ij} = \left(\frac{\mathrm{d}^2E}{\mathrm{d}\mathbf{F}_i\,\mathrm{d}\mathbf{F}_j}\right)_{\mathbf{F}=0}$$

When a molecular system is subjected to a fluctuating electric field, $\mathbf{F} = \mathbf{r}\cos(\omega t)$, (r is the position vector in one dimension, t is the time and ω is the frequency of fluctuation) the frequency dependent polarizability (i.e., dynamic polarizability) may be expressed as

$$\langle\alpha\rangle_\omega = \sum_{i\neq 0}^{\text{states}} \frac{|\langle\psi_0|r|\psi_i\rangle|^2}{\omega - (E_i - E_0)}$$

where the numerator of each term in the sum is the transition dipole moment and the denominator involves the frequency (ω) and energy of the excited (E_i) and ground states (E_0), respectively. All these calculations have been carried out applying a general *ab initio* quantum chemistry software, GAMESS on a PC based LINUX cluster platform.[24] Triple split Gaussian type basis sets for Br and I atoms and Sadlej basis sets for all the atoms are obtained from the Extensible Computational Chemistry Environment Basis Set Database, Pacific Northwest Laboratory. The calculations are carried out by reading external basis set file as implemented in GAMESS. Visualization of molecular systems has been carried out by MOLDEN program.[25]

3. Results and Discussion

3.1. Structure. Geometry optimization of mono- and dihydrated clusters of Cl_2 and Br_2 has been carried out at MP2, BHHLYP, and B3LYP levels of theory by applying triple split valence basis set adding polarization as well diffusion functions. Calculated bond distances and static polarizability parameters are listed in Table 1. It is noticed that B3LYP functional predicts longer bond lengths compared to MP2 values whereas BHHLYP functional predicts shorter bond lengths in all the cases. Calculated bond distances applying BHHLYP density functional are closer to MP2 values than the same calculated following B3LYP density functional. Similar results are also observed in the case of the calculated static polarizability of these hydrated clusters. On the basis of these observations, all the calculations are carried out applying correlated hybrid density functional, namely, BHHLYP.

TABLE 1: Calculated Geometrical Parameter and Polarizability of $X_2 \cdot nH_2O$ Systems (X = Cl and Br; n = 1−2) at Various Levels of Theory Using the 6-311++G(d,p) Basis Set[a]

	X−X distance (Å)		X···O distance[b] (Å)		static polarizability (au)	
method	X = Cl	X = Br	X = Cl	X = Br	X = Cl	X = Br
			$X_2 \cdot H_2O$			
MP2	2.031	2.319	2.799	2.830	29.75	44.16
BHHLYP	2.027	2.310	2.742	2.785	29.67	43.93
B3LYP	2.066	2.345	2.712	2.762	30.80	45.10
			$X_2 \cdot 2H_2O$			
MP2	2.038	2.324	2.707	2.747	38.12	52.44
BHHLYP	2.036	2.313	2.646	2.731	38.11	52.09
B3LYP	2.092	2.349	2.549	2.702	40.47	53.47

[a] The polarizability is calculated at the TDHF/6-311++G(d,p) level with the optimized geometry. [b] X···O distance refers to the minimum X···O separation.

Solvent H_2O molecules are added to Cl_2, Br_2, and I_2 species by various different possible ways and full geometry optimization is carried out at BHHLYP/6-311++G(d,p) level (6-311 basis set is used for I) of theory followed by single point energy calculation at second-order Moller−Plesset perturbation theory (MP2) with the same basis set. Optimized structures of the most stable configurations for each size hydrated cluster of Cl_2, Br_2, and I_2 systems are displayed in Figure 1. Structures corresponding to IA, IB, and IC are the most stable structures of the monohydrate clusters, $Cl_2 \cdot H_2O$, $Br_2 \cdot H_2O$, and $I_2 \cdot H_2O$. For all the structures, O atom from H_2O molecule is connected to one of the halogen atoms ($r_{O\cdots X} \sim 2.5$ Å). Most favored structures for dihydrated cluster of Cl_2, Br_2, and I_2 systems are shown as IIA, IIB, and IIC, respectively, in Figure 1. It is clearly observed that only one H_2O molecule is in the close vicinity of halogen moiety in the dihydrated clusters except for $Br_2 \cdot 2H_2O$ cluster, where both water molecules are in the close vicinity of Br_2. It is to be noted that the initial guess structures for dihydrated clusters were considered where one H_2O molecule attached to one of the halogen atoms (Cl, Br, or I) through the O site and the other H_2O is connected to X_2 via the H atom without any inter-water H bonding. Structures of the most stable configurations of trihydrated cluster of Cl_2, Br_2, and I_2 are very similar in nature and are displayed in Figure 1 as IIIA, IIIB, and IIIC, respectively. Two solvent water molecules are in close proximity and connected by H-bonds in these trihydrate clusters. The initial guess structures were considered where all the three solvent H_2O units were directly linked to halogen atoms. In the case of the tetrahydrated cluster, planar cyclic H-bonded structures (see Figure 1 IVA, IVB, and IVC) are obtained as the most stable geometries. One can see that only two solvent water molecules are directly connected to the halogen atoms and the remaining two act as both H-bond donor and acceptor in this minimum energy structure. In the case of pentahydrated clusters, the most favored structures are also planar where the H atom of one H_2O is approached by one halogen (Cl, Br, or I) atom and the O atom of another H_2O is approached by another halogen atom

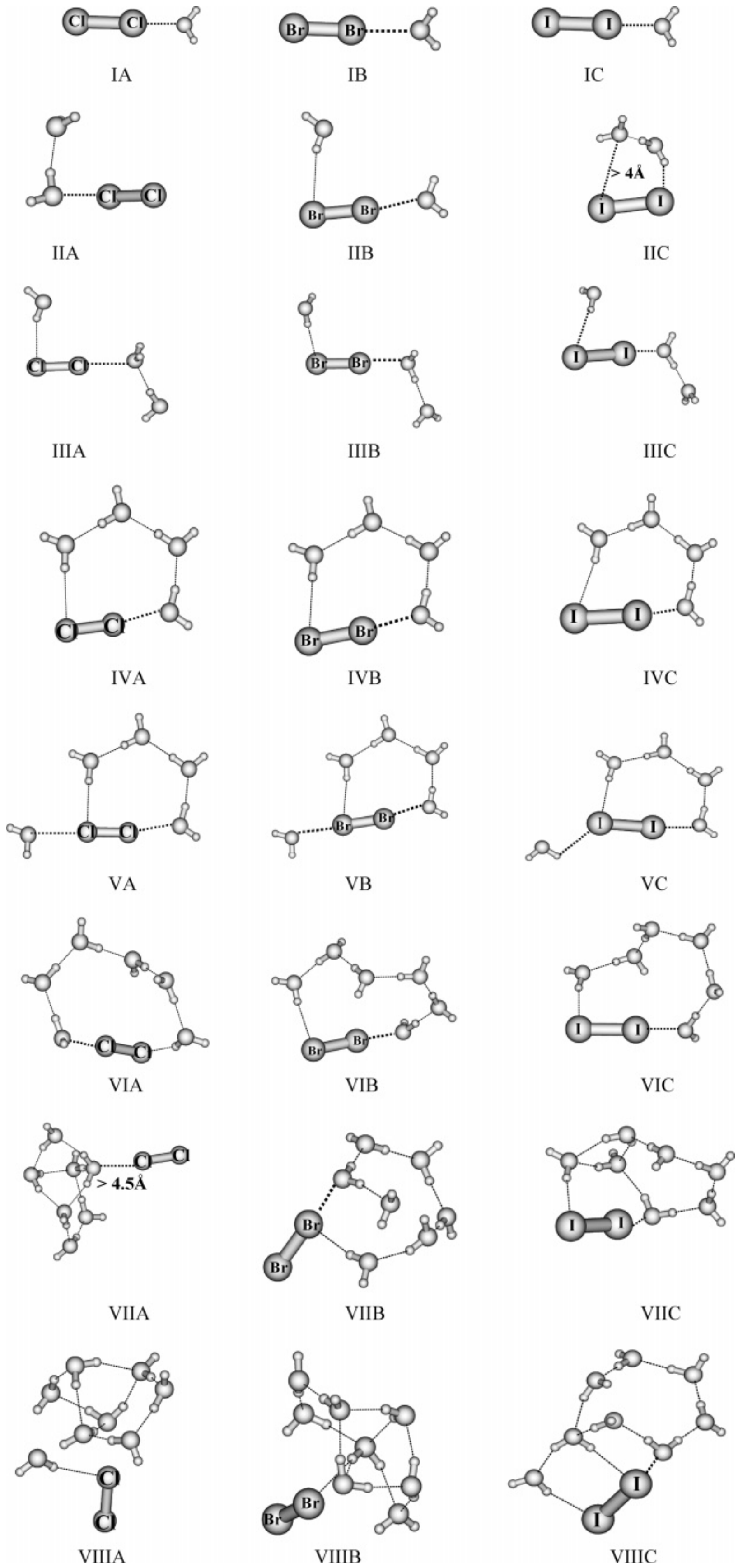

Figure 1. Fully optimized most stable structures calculated by applying the BHHLYP functional with the 6-311++G(d,p) set of split valence basis function (6-311 basis set is used for iodine) for (IA) $Cl_2\cdot H_2O$, (IB) $Br_2\cdot H_2O$, (IC) $I_2\cdot H_2O$, (IIA) $Cl_2\cdot 2H_2O$, (IIB) $Br_2\cdot 2H_2O$, (IIC) $I_2\cdot 2H_2O$, (IIIA) $Cl_2\cdot 3H_2O$, (IIIB) $Br_2\cdot 3H_2O$, (IIIC) $I_2\cdot 3H_2O$, (IVA) $Cl_2\cdot 4H_2O$, (IVB) $Br_2\cdot 4H_2O$, (IVC) $I_2\cdot 4H_2O$, (VA) $Cl_2\cdot 5H_2O$, (VB) $Br_2\cdot 5H_2O$, (VC) $I_2\cdot 5H_2O$, (VIA) $Cl_2\cdot 6H_2O$, (VIB) $Br_2\cdot 6H_2O$, (VIC) $I_2\cdot 6H_2O$, (VIIA) $Cl_2\cdot 7H_2O$, (VIIB) $Br_2\cdot 7H_2O$, (VIIC) $I_2\cdot 7H_2O$, (VIIIA) $Cl_2\cdot 8H_2O$, (VIIIB) $Br_2\cdot 8H_2O$, and (VIIIC) $I_2\cdot 8H_2O$. Cl, Br, and I atoms are shown by marked spheres; the smallest spheres refer to H atoms, and the rest correspond to O atoms in each structure.

and both these H_2O units are linked with two other solvent H_2O molecules via H-bond. The fifth solvent unit is connected to the halogen atom (which is already connected by a H_2O unit through the H atom) through its O atom in the case of $Cl_2\cdot 5H_2O$ and $Br_2\cdot 5H_2O$ systems and through one of its H atoms in the $I_2\cdot 5H_2O$ system, as shown in Figure 1 (VA, VB, and VC). It is to be noted that in all these three cases the initial structure for optimization was similar. The most stable structure for hexahydrated cluster, $Cl_2\cdot 6H_2O$ is calculated to have a surface structure with a three-dimensional water network formed by six H_2O molecules via inter-water H-bonding, as displayed in Figure 1 VIA. The minimum energy structure of the $Br_2\cdot 6H_2O$ and $I_2\cdot 6H_2O$ clusters (see Figure 1 VIB and VIC) is similar to that of the $Cl_2\cdot 6H_2O$ cluster. In the case of the heptahydrated cluster, the Cl_2 system behaves in a different manner compared to that of the Br_2 and I_2 systems. The most stable structures of $Cl_2\cdot 7H_2O$, $Br_2\cdot 7H_2O$, and $I_2\cdot 7H_2O$ are shown in Figure 1 (VIIA, VIIB, and VIIC). In the $Cl_2\cdot 7H_2O$ cluster, the solvent water units are separated from the Cl_2 moiety by a distance of ~4.0 Å. The most favored structure of $Br_2\cdot 7H_2O$ is the one where the three-dimensional network surrounds only one Br atom (see Figure 1 VIIB). On the other hand, the most stable structure of the $I_2\cdot 7H_2O$ cluster is the one where the I_2 unit is surrounded by a cyclic three-dimensional water network formed by seven H_2O molecules via an inter-water H-bond, as shown in Figure 1 VIIC. All the H_2O molecules act as both H-bond donor and acceptor in this heptahydrated cluster except the two, which were directly attached to the I_2 moiety. The most stable structure of the $Cl_2\cdot 8H_2O$ cluster is displayed in Figure 1 VIIIA. It is clearly seen that the Cl_2 moiety is directly attached to only one water molecule as the monohydrated system, $Cl_2\cdot H_2O$, and staying away (>4 Å) from the seven-member water network. The most stable structure of the $Br_2\cdot 8H_2O$ cluster (see Figure 1 VIIIB) is rather different from that of $Br_2\cdot 7H_2O$ cluster (see Figure 1 VIIB). In the present case, all the water molecules act simultaneously as hydrogen bond donors and acceptors except the water molecule directly attached to the bromine moiety by the H-end. The minimum energy structure of the $I_2\cdot 8H_2O$ cluster is very similar to that from the heptahydrated cluster, $I_2\cdot 7H_2O$. All eight water molecules form a cyclic network, which is connected to the iodine molecule from one side of I_2 making a surface structure as shown in Figure 1 VIIIC.

All $X_2\cdot nH_2O$ (X = Cl, Br, and I; $n = 1-8$) clusters are stabilized by X···O, X···H, and inter-water hydrogen bonding interactions. The inter-water hydrogen-bonding energy (~6−7 kcal/mol) is greater than the both X···O and X···H interaction energies (~3−5 kcal/mol). Thus, the larger clusters prefer to form a strong inter-water hydrogen-bonded network. The structures of all these systems are widely different for the larger size clusters ($n > 6$) though they are fairly similar in the case of smaller clusters ($n = 1-6$) except for $n = 2$. The structures of $Br_2\cdot nH_2O$ ($n = 7, 8$) clusters are quite different from the earlier reported work at a lower level of theory.[16]

3.2. Atomic Charge and Bond Order. The calculated Mulliken atomic charges over two Br atoms in $Br_2\cdot H_2O$ cluster are ~0.04 and −0.08 au. A small variation on atomic charge over two Br atoms is observed for different size hydrated clusters, $Br_2\cdot nH_2O$ and observed to be in the range 0.04−0.14 au. This suggests that Br_2 exists as a charge-separated ion-pair species ($Br^{\delta+}-Br^{\delta-}$) in the studied hydrated clusters. For the $I_2\cdot H_2O$ cluster, the calculated Mulliken atomic charges over two I atoms are ~0.03 and −0.16 au. The variation on atomic charge over two I atoms for different size hydrated clusters, $I_2\cdot nH_2O$ is observed to be larger than that of Br atoms in $Br_2\cdot nH_2O$ cluster. This suggests that I_2 does exist as a charge-separated ion-pair species ($I^{\delta+}-I^{\delta-}$) in the studied hydrated clusters like Br_2 in $Br_2\cdot nH_2O$ systems. However, in contrast to I_2 and Br_2 systems, Cl_2 does not exist as a charge separated species in presence of solvent water molecules. The calculated Mulliken charges over two Cl atoms are fairly close (+0.01 and −0.04 au). This may be due to the high electronegativity of Cl atom compared to Br and I atoms. It is worth mentioning that no charge separation is observed in the case of mono- and dihydrated F_2 cluster, F being the highest electronegative element in this row F > Cl > Br > I. This observation may be due to the fact that there is a competition between ion solvation force, which favors a localized charge distribution and chemical bond interaction, which tend to delocalize a charge. As one moves from Cl_2 to Br_2 to I_2, the bond gets longer and weaker. As a result, at some stage the charge-separated form becomes more stable than the delocalized form. In other words, the cost to form charge-separated ion pair is large in the case of $Cl_2\cdot nH_2O$ system compared to $Br_2\cdot nH_2O$ or $I_2\cdot nH_2O$ systems due to relatively large ionization potential. It is known that the Mulliken charge is sensitive to the basis function applied in the calculation. Thus, atomic charges are also calculated applying atoms in molecules (AIM) based procedure at the BHHLYP/6-311G(d,p) level of theory. The predicted charge separation between two halogen atoms is 0.03, 0.09, 0.13, and 0.19 for $F_2\cdot H_2O$, $Cl_2\cdot H_2O$, $Br_2\cdot H_2O$, and $I_2\cdot H_2O$ systems, respectively at listed in Table 2. The charge-separation values calculated by AIM procedure show the similar trend as calculated Mulliken charges do. The effect of basis set is also tested on these systems for AIM charge-separation values and the results are supplied in Table 2. It is noticed that calculated AIM charge-separation values become smaller with the inclusion of larger basis functions. Bond orders between the two halogen atoms for all the clusters ($X_2\cdot nH_2O$; X = Cl and I; $n = 1-8$) are also calculated following the definition due to Mayer.[26] The calculated bond distance (r_{xx}) and bond order (B_{xx}) between two halogen atoms do not show any significant variation on addition of successive solvent water molecules. From the structural information it is noted that only a few water molecules are in close surrounding of halogen (X_2) moiety.

TABLE 2: Calculated Charge Separation between Two Halogen Atoms in the $X_2\cdot H_2O$ Cluster Following Natural Population Analysis at the BHHLYP Level of Theory Adopting Different Sets of Basis Functions

basis set	charge separation between two halogen atoms (X−X) (au)			
	$F_2\cdot H_2O$	$Cl_2.H_2O$	$Br_2.H_2O$	$I_2\cdot H_2O$
6-311G	0.05	0.12	0.17	0.23
6-311G(d,p)	0.03	0.09	0.13	0.19
6-311++G(d,p)	0.02	0.08	0.13	*a*

[a] Basis set 6-311+G(d) is not available for I atom.

3.3. Stabilization and Interaction Energy. Stabilization energy of these clusters $X_2\cdot nH_2O$ (X = Cl, Br, and I) may be expressed as $E^{\text{stab}} = E_{X_2\cdot\, nH_2O} - (nE_{H_2O} + E_{X_2})$, where $E_{X_2\cdot nH_2O}$ refers to the energy of the cluster $X_2\cdot nH_2O$ (X = Cl, Br, and I). E_{H_2O} and E_{X_2} refer to the energy of a single H_2O and X_2 (X = Cl, Br, and I) system. Thus, the calculated stabilization energy represents the stabilization of the molecular cluster on addition of successive solvent water molecules accounting interaction of halogen atoms with water units as well as inter-water H-bonding. The stabilization energy of the $X_2\cdot nH_2O$ (X = Cl, Br, and I) clusters calculated at the MP2/6-311++G(d,p) level of theory (for I the 6-311 basis is used) are provided in Table 3. The variation of solvation energy (E^{stab}) vs n (the number of

TABLE 3: Calculated Stabilization and Interaction Energy in kcal/mol for $X_2\cdot nH_2O$ Systems (X = Cl, Br, and I; *n* = 1−8) at the MP2/6-311++G(d,p) Level of Theory[a]

	stabilization energy of $X_2\cdot nH_2O$ clusters (kcal/mol)			interaction energy of $X_2\cdot nH_2O$ clusters (kcal/mol)		
$X_2.nH_2O$	X = Cl	X = Br	X = I	X = Cl	X = Br	X = I
$n = 1$	2.85	3.86	4.57	3.07	4.11	4.88
$n = 2$	9.85	5.52	8.42	4.36	5.76	3.00
$n = 3$	9.88	13.53	16.31	3.91	7.74	10.80
$n = 4$	25.82	27.68	32.18	7.42	9.58	14.59
$n = 5$	28.24	30.23	33.69	8.49	11.02	15.76
$n = 6$	45.66	47.87	52.70	9.31	11.66	16.48
$n = 7$	65.00	60.03	67.40	4.55	11.32	23.40
$n = 8$	73.25	71.26	76.71	6.57	13.73	23.11

[a] 6-311 basis set is applied for the I atom.

water molecules in a $X_2\cdot nH_2O$ cluster (X = Cl, Br, and I)) are displayed in Figure 2A−C, respectively, showing a continuous increase on addition of each solvent water units.

It is clearly seen from Table 3 that the stabilization energy is the highest for the $I_2\cdot nH_2O$ system. But between $Cl_2\cdot nH_2O$ and $Br_2\cdot nH_2O$ systems the stabilization energy does not follow any systematic trend; variation is different for different cluster sizes (*n*) of the $Cl_2\cdot nH_2O$ and $Br_2\cdot nH_2O$ systems. It is known that the solubility of the Br_2 gas is higher than that for the Cl_2 gas in bulk water. Thus, the calculated stabilization cannot explain the solubility of the halogen (Cl_2, Br_2, and I_2) in water. Let us introduce another energy term known as the interaction energy.

The interaction energy (E^{int}) between the halogen (X_2) and water cluster in the hydrated cluster, $X_2\cdot nH_2O$ (X = Cl, Br, and I) may be defined as $E^{int} = E_{X_2\cdot nH_2O} - (E_{(H_2O)n} + E_{X_2})$, where, $E_{X_2\cdot nH_2O}$ refers to the energy of the cluster $X_2\cdot nH_2O$ (X = Cl and I). $E_{(H_2O)n}$ and E_{X_2} refer to the energy of $(H_2O)_n$ and X_2 (X = Cl, Br and I) systems, respectively. The energy of the $(H_2O)_n$ system is calculated by removing halogen (X_2) part from the optimized geometry of the cluster followed by a single point energy calculation. E_{X_2} is also evaluated in the similar way, i.e., by removing the water part of the optimized structure of hydrated cluster followed by single point energy calculation. Thus, the interaction energy actually calculates the net interaction of X_2 with $(H_2O)_n$ systems in these hydrated clusters. The interaction energy of the $X_2\cdot nH_2O$ (X = Cl, Br, and I) clusters calculated at the MP2/6-311++G(d,p) level of theory are listed in Table 3. As expected, the calculated interaction energy is very small compared to the same calculated for charged systems, $X_2^{\bullet-}\cdot nH_2O$.[14,16] Moreover, it can be easily seen from Table 3 that the interaction energy for $Cl_2\cdot nH_2O$ systems is quite small with respect to Br_2 and I_2 hydrated systems. This does support the presence of Br_2 and I_2 as charge separated ion pair in the hydrated clusters. The plot of calculated interaction energy (E^{int}) vs *n* (the number of water molecules for $Cl_2\cdot nH_2O$ and $I_2\cdot nH_2O$ clusters) are displayed in Figure 2A−C, respectively. The interaction energy for hepta- and octahydrated clusters of Cl_2 systems is smaller than that for a hexahydrated cluster. This may be due to the specific geometry of the hydrated clusters where seven solvent water molecules form a H-bonded cluster that remains far away from the Cl_2 moiety. For $Br_2\cdot nH_2O$ clusters, the calculated interaction energy profile shows saturation at $n = 7$. In the case of $I_2\cdot nH_2O$ clusters, the calculated interaction energy profile shows a stepwise saturation nature at $n = 6$ and 8.

The interaction energy (E^{int}) is the measure of the interaction between halogen moiety and water units. Thus, a large value of E^{int} indicates the presence of a large number of water molecules in close surrounding of the halogen moiety. For the present systems, calculated E^{int} is small and shows only a small increase with the addition of water molecules. That explains the presence of only a few water molecules (two to three) in the close vicinity of the halogen moiety. It is to be noted that the calculated interaction energy is much higher in the presence of an excess electron in such systems.[14,16] In the case of hydrated clusters, $X_2\cdot nH_2O$ (X = Cl, Br, and I; $n = 1-8$), the stabilization and interaction energy are very close for a few small size clusters. But when an intermolecular hydrogen bond among water molecules starts to build up, the solvation energy surpasses the interaction energy. The variation of stabilization energy with size of the cluster (*n*) for all the systems is similar. On the other hand, variation of interaction energy with size of the cluster (*n*) is different for Cl_2 system compared to that of Br_2 and I_2 system.

Table 3 indicates that the interaction energy decreases from $I_2\cdot nH_2O$ to $Cl_2\cdot nH_2O$ systems for all sizes of the clusters except for $n = 2$. Thus the calculated interaction energy in these halogen−water clusters should be able to predict the solubility of X_2 in water. A calculated higher interaction energy for $Br_2\cdot nH_2O$ clusters than that for $Cl_2\cdot nH_2O$ cluster is able to explain the higher solubility of bromine in bulk water over chlorine. As $I_2\cdot nH_2O$ possesses the highest interaction energy among these three systems, iodine in the gas phase is expected to have a much higher solubility in bulk water compared to bromine and chlorine gases.

3.4. Static and Dynamic Polarizabilities. The knowledge about the response of these hydrated clusters to an external electric field is important for understanding intermolecular interaction. Linear response properties are characterized by the polarizability. Static and dynamic polarizabilities of these hydrated clusters are calculated with the most stable structures of $X_2\cdot nH_2O$ clusters (X = Cl, Br, and I) following the time dependent Hartree Fock (TDHF) method. The dynamic polarizability of the clusters is calculated by applying an external field frequency (ω) of 0.05 au. Static ($\omega = 0$) and dynamic ($\omega = 0.05$ au) polarizabilities of $Cl_2\cdot nH_2O$ clusters ($n = 1-8$) are calculated with a spilt valence Gaussian basis function, 6-311++G(d,p) and supplied in Table 4. The variation of the static ($\omega = 0$) polarizability with the size (*n*) of hydrated clusters of Cl_2 is shown in Figure 3a. A similar variation for the dynamic polarizability ($\omega = 0.05$ au) of $Cl_2\cdot nH_2O$ clusters is displayed in Figure 4a. It is clearly seen from the figures that the variation of polarizability (α) with the successive addition of solvent water units is linear. The calculated static polarizability (α_0) is observed to be best fitted as $\alpha_0 = 22.04 + 7.80n$, where *n* is the number of water molecules present in the cluster. The calculated dynamic polarizability with the external field of frequency 0.05 au ($\alpha_{0.05}$) is best fitted by the equation, $\alpha_{0.05} = 22.35 + 7.86n$. Both these fitted linear equations have correlation coefficients >0.999. The static ($\omega = 0$) and dynamic ($\omega = 0.05$ au) polarizabilities of $Br_2\cdot nH_2O$ clusters ($n = 1-8$) are also calculated at the same level of theory and tabulated in Table 4. The variation of polarizabilities with the size (*n*) of the clusters at $\omega = 0$ (static) and $\omega = 0.05$ au are shown in Figures 3b and 4b, respectively. The variation of static and dynamic polarizabilities (α_0) vs cluster size (*n*) are linear and best fitted with the equations $\alpha_0 = 35.47 + 8.37n$ and $\alpha_{0.05} = 36.02 + 8.45n$, respectively. These linear fittings also have correlation coefficients >0.999, showing the reliable predictability for the polarizability of larger size clusters. Polarizabilities of $I_2\cdot nH_2O$ clusters ($n = 1-8$) are also calculated at TDHF level with the 6-311G set of basis function for I and 6-311++G(d,p) basis functions for O and H atoms. The calculated polarizabilities of

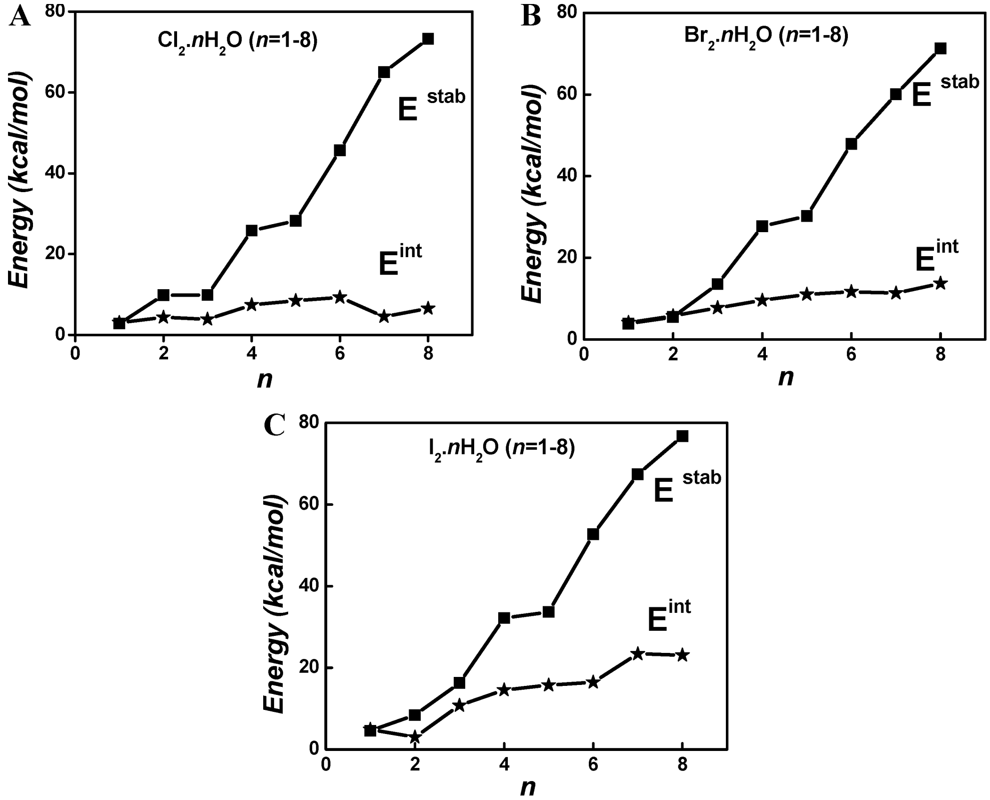

Figure 2. Plot of calculated interaction energy, E^{int}, and stabilization energy, E^{stab}, at the MP2/6-311++G(d,p) level in kcal/mol vs n, number of water molecules for (A) $Cl_2 \cdot nH_2O$, (B) $Br_2 \cdot nH_2O$, and (C) $I_2 \cdot nH_2O$ clusters.

TABLE 4: Calculated Static and Dynamic Polarizabilities (in au) with the External Field Frequency of 0.05 au ($\omega = 0.05$ au) for $X_2 \cdot nH_2O$ Clusters (X = Cl, Br, and I; $n = 1-8$) at the TDHF Level of Theory Considering Split Valence 6-311++G(d,p) (6-311 Basis Set for I) and Sadlej Basis Sets

	static polarizability (au) of $X_2 \cdot nH_2O$ clusters[a]			dynamic polarizability (au) of $X_2 \cdot nH_2O$ clusters at external field frequency (ω) = 0.05 au[a]		
$X_2 \cdot nH_2O$	X = Cl	X = Br	X = I	X = Cl	X = Br	X = I
$n = 1$	29.67 (40.06)	43.93 (54.48)	56.86 (87.08)	30.02 (40.46)	44.56 (55.20)	58.66 (89.05)
$n = 2$	38.11 (49.34)	52.09 (62.94)	63.81 (96.06)	38.55 (49.84)	52.79 (63.72)	65.43 (91.79)
$n = 3$	44.56 (57.00)	61.13 (73.04)	80.12 (107.33)	45.02 (57.51)	61.96 (73.96)	82.43 (109.68)
$n = 4$	53.65 (66.37)	69.02 (81.37)	88.63 (115.50)	54.20 (66.97)	79.90 (82.33)	90.96 (117.87)
$n = 5$	60.67 (75.05)	76.06 (90.09)	96.65 (123.91)	61.25 (75.71)	76.97 (91.10)	99.04 (126.31)
$n = 6$	70.36 (83.92)	86.01 (99.35)	106.11 (133.42)	71.05 (84.67)	87.06 (100.48)	108.67 (136.0)
$n = 7$	75.95 (90.95)	94.37 (108.34)	118.48 (142.86)	76.63 (91.70)	95.51 (109.57)	121.4 (145.74)
$n = 8$	84.21 (99.16)	102.50 (115.60)	127.52 (152.71)	84.95 (99.96)	103.71 (116.90)	130.56 (155.70)

[a] Values in parentheses refer to the data calculated by applying the Sadlej basis set.

$I_2 \cdot nH_2O$ clusters are listed in Table 4. The linear variation of polarizabilities with the size of the clusters at $\omega = 0$ (static) and $\omega = 0.05$ au are shown in Figures 3c and 4c, respectively. The best-fitted equations are $\alpha_0 = 46.52 + 10.17n$ and $\alpha_{0.05} = 48.04 + 10.36n$, respectively, for static and dynamic polarizabilities with a correlation coefficient >0.996.

Static ($\omega = 0$) and dynamic ($\omega = 0.05$ au) polarizabilities are also calculated with the Sadlej basis function as this particular basis set especially designed for accurate calculation of polarizability,[27] and the calculated results are given in Table 4. For $Cl_2 \cdot nH_2O$ clusters ($n = 1-8$), the best-fitted linear equations are $\alpha_0 = 32.13 + 8.47n$ and $\alpha_{0.05} = 32.49 + 8.52n$, respectively, for static and dynamic polarizabilities at the external field frequency (ω) of 0.05 au. Best-fitted linear equations for the variation of static ($\omega = 0$) and dynamic ($\omega = 0.05$ au) polarizabilities of $Br_2 \cdot nH_2O$ clusters ($n = 1-8$) are $\alpha_0 = 45.88 + 8.84n$ and $\alpha_{0.05} = 46.51 + 8.92n$, respectively. In the case of hydrated clusters of I_2, the best-fitted linear equations are $\alpha_0 = 78.07 + 9.29n$ and $\alpha_{0.05} = 77.39 + 9.81n$, respectively, for static and dynamic polarizabilities ($\omega = 0.05$ au). All these linear fit plots have correlation coefficient >0.999. Thus, for all the systems $X_2 \cdot nH_2O$ (X = Cl, Br, and I; $n = 1-8$) both static and dynamic polarizabilities vary linearly with the size (n) of the cluster at the TDHF level of theory with Sadlej as well as the 6-311++G(d,p) set of basis functions. This suggests that a simple additive effective polarizability model can predict the polarizability of larger hydrated clusters. The linear plots of calculated static polarizability vs cluster size (n) exhibit slopes of 8.47, 8.92, and 9.29 au adopting the Sadlej basis function compared to the slopes of 7.80, 8.37, and 10.17 au adopting the Gaussian basis function for hydrated clusters of Cl_2, Br_2, and I_2, respectively. This means that the increase in polarizability for each additional solvent water unit (slope of line) is more with the Sadlej basis function compared to the same with Gaussian type basis function except for $I_2 \cdot nH_2O$ system. The calculated slopes also suggest that the increase in polarizability for each additional solvent water unit goes in the order $I_2 > Br_2 > Cl_2$. This is because polarizabilities of these systems are also in the order $I_2 > Br_2 > Cl_2$ due to their size. Similar results

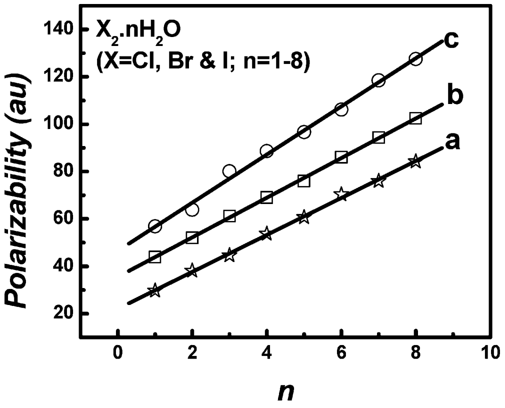

Figure 3. Plot of calculated static polarizability (au) at TDHF/6-311++G(d,p) level for the hydrated clusters (a) $Cl_2 \cdot nH_2O$, (b) $Br_2 \cdot nH_2O$, and (c) $I_2 \cdot nH_2O$ against the number of solvent water units (*n*) present in the clusters.

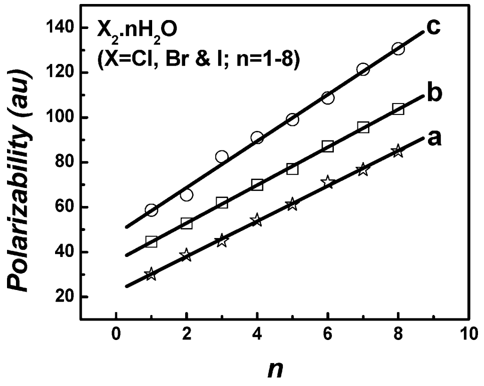

Figure 4. Plot of calculated dynamic polarizability (au) at TDHF/6-311++G(d,p) level for the hydrated clusters (a) $Cl_2 \cdot nH_2O$, (b) $Br_2 \cdot nH_2O$, and (c) $I_2 \cdot nH_2O$ against the number of solvent water units (*n*) present in the clusters in presence of an external field of frequency (ω) 0.05 au.

are observed in the case of the calculated dynamic polarizability of these systems.

It is known that the dynamic polarizability of atomic or molecular systems increases sharply if the applied external field is in the close vicinity of electronic transition of the system. It will be interesting to see how the polarizability (α) varies with the frequency (ω) of the external field in these clusters. Hydrated clusters $X_2 \cdot H_2O$ and $X_2 \cdot 4H_2O$ (X = Cl, Br, and I) are considered for such study. The polarizability (α) of $X_2 \cdot H_2O$ and $X_2 \cdot 4H_2O$ clusters (X = Cl, Br, and I) is calculated for $\omega = 0$ to 0.10 au with a span of 0.01 au at TDHF level with 6-311++G(d,p) set of basis function (6-311 basis set for I). The variation of polarizability (α) with frequency (ω) of the external field is shown in Figure 5 for $X_2 \cdot H_2O$ (X = Cl, Br, and I) clusters. It is observed that the polarizability of these hydrated clusters grows exponentially with the application of an external field. For monohydrated clusters, the variation of polarizability with the external field can be expressed as $\alpha = 29.41 + 0.22 \exp(\omega/0.05)$, $\alpha = 43.49 + 0.37 \exp(\omega/0.05)$ and $\alpha = 55.74 + 0.93 \exp(\omega/0.04)$ for Cl_2, Br_2, and I_2 systems, respectively, with χ^2 values ~0.0015. For tetrahydrated clusters, the variation of polarizability with the external field can be expressed as $\alpha = 53.25 + 0.34 \exp(\omega/0.05)$, $\alpha = 68.40 + 0.52 \exp(\omega/0.05)$, and $\alpha = 87.27 + 1.14 \exp(\omega/0.04)$ for Cl_2, Br_2, and I_2 systems, respectively, with χ^2 values <0.02. Polarizability (α) is also calculated for $\omega = 0.0-0.10$ au with a span of 0.01 au at the TDHF level of theory with the Sadlej basis set. The calculated polarizability profiles with the external field are very similar to those with the split valence Gaussian basis set. The best fitted equations are $\alpha = 39.77 + 0.25 \exp(\omega/0.05)$, $\alpha = 53.99 + 0.42 \exp(\omega/0.05)$, and $\alpha = 86.05 + 0.53 \exp(\omega/0.03)$, respectively, for $Cl_2 \cdot H_2O$, $Br_2 \cdot H_2O$, and $I_2 \cdot H_2O$ clusters with χ^2 values less than 0.02. On the other hand, the best-fitted equations are $\alpha = 65.93 + 0.37 \exp(\omega/0.05)$, $\alpha = 80.69 + 0.57 \exp(\omega/0.05)$, and $\alpha = 114.15 + 1.09 \exp(\omega/0.04)$, respectively, for $Cl_2 \cdot 4H_2O$, $Br_2 \cdot 4H_2O$, and $I_2 \cdot 4H_2O$ clusters with χ^2 values less than 0.02. One may notice that the increase in dynamic polarizability is much smaller in the case of the Cl_2 hydrated cluster as the applied external field (2.72 eV) is much lower than the energy required for first electronic transition in this system. However, in the case of the I_2 hydrated cluster, the increase in dynamic polarizability is quite large as the applied external field is close to the energy required for the first electronic transition in this system. In general, the dynamic polarizability profiles of these hydrated clusters behave in the same fashion as in the case of atom or molecules.

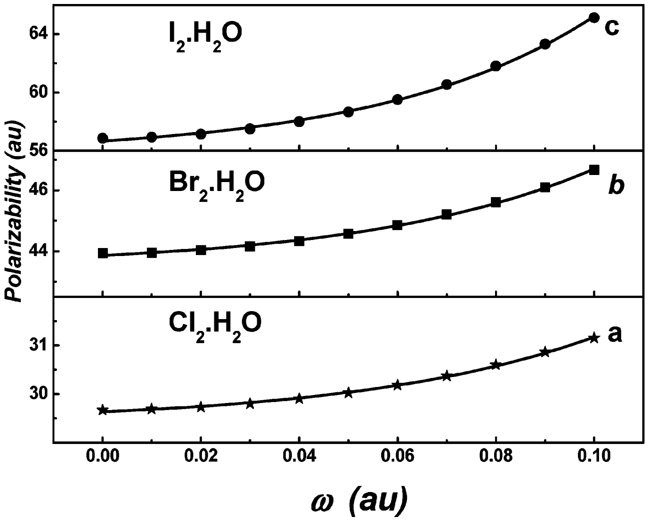

Figure 5. Plot of calculated polarizability (au) vs ω, frequency of the external field (au) for the monohydrated clusters (a) $Cl_2 \cdot H_2O$, (b) $Br_2 \cdot H_2O$, and (c) $I_2 \cdot H_2O$ at TDHF/6-311++G(d,p) level.

4. Conclusions

The structure, energy, and polarizability for hydrated halogen clusters, $X_2 \cdot nH_2O$ (X = Cl, Br, and I) are reported. Both *ab initio* (MP2) and hybrid exchange–correlation functionals, namely, BHHLYP, have been applied to study the present systems with a split valence 6-311++G(d,p) basis function. Various initial guess structures are taken for each size cluster for geometry optimization to find out different minimum energy configurations. Several closely spaced minimum energy structures are predicted on the basis of a quasi-Newton search. Single point energy calculation has been carried out at the MP2 level with the same basis set for correction of energy term by considering the electron correlation in a better way. It is concluded that both Br_2 and I_2 exist as a charge separated ($Br^{+\delta}-Br^{-\delta}$ and $I^{+\delta}-I^{-\delta}$) entity in the hydrated clusters. Though structures of $Cl_2 \cdot nH_2O$ clusters are similar to that of the iodine system, Cl_2 does not exist as a charge separated ion pair in the presence of solvent water units. The interaction and stabilization energy are calculated for $X_2 \cdot nH_2O$ clusters (X = Cl, Br, and I; $n = 1-8$). The calculated stabilization energy increases on successive addition of solvent water molecules but interaction energy saturates for all three halogen-hydrated systems. The higher interaction energy and charge distribution over the I atom in $I_2 \cdot nH_2O$ clusters compared to that of $Br_2 \cdot$

nH$_2$O and Cl$_2$•nH$_2$O clusters suggests that the solubility of gas-phase I$_2$ is higher than those for Br$_2$ and Cl$_2$ gases. Response properties like static and dynamic polarizabilities of X$_2$•nH$_2$O clusters (X = Cl, Br, and I; $n = 1-8$) are calculated following time dependent Hartree−Fock (TDHF) theory by applying triple split valence as well as Sadlej basis sets. Both static and dynamic polarizabilities vary linearly with the size of the clusters (n) for X$_2$•nH$_2$O cluster systems. It is noted that the calculated polarizability grows exponentially with the frequency of the external applied field for any size of hydrated clusters studied.

Acknowledgment. We thank the computer center, BARC, for providing the ANUPAM parallel computing facility. We are also thankful to Dr. S. K. Ghosh for many helpful discussions. Dr. S. K. Sarkar is gratefully acknowledged for encouragement.

References and Notes

(1) Marcus, Y. *Chem. Rev.* **1988**, *88*, 1475.

(2) Illenberger, E. *Chem. Rev.* **1992**, *92*, 1589.

(3) Ohtaki, H.; Radani, T. *Chem. Rev.* **199**3, *93*, 1157.

(4) Simons, J.; Jordan, K. D. *Chem. Rev.* **1987**, *87*, 535.

(5) (a) Majumdar, D.; Kim, J.; Kim, K. S. *J. Chem. Phys.* **2000**, *112*, 101. (b) Kim, J.; Lee, H. M.; Suh, S. B.; Majumdar, D.; Kim, K. S. *J. Chem. Phys.* **2000**, *113*, 5259. (c) Lee, H. M.; Kim, D.; Kim, K. S. *J. Chem. Phys*. **2002**, *116*, 5509.

(6) (a) Ayala, R.; Martinez, J. M.; Pappalardo, R. R.; Marcos, E. S. *J. Chem. Phys.* **2003**, *119*, 9538. (b) Ayala, R.; Martinez, J. M.; Pappalardo, R. R.; Marcos, E. S. *J. Phys. Chem. A* **2000**, *104*, 2799. (c) Ayala, R.; Martinez, J. M.; Pappalardo, R. R.; Saint-Martin, H.; Ortega-Blake, I.; Marcos, E. S. *J. Chem. Phys*. **2002**, *117*, 10512. (d) Ayala, R.; Martinez, J. M.; Pappalardo, R. R.; Marcos, E. S. *J. Chem. Phys.* **2004**, *121*, 7269.

(7) Bryce, R. A.; Vincent, M. A.; Malcolm, N. O. J.; Hillier, I. H. *J. Chem. Phys.* **1998**, *109*, 3077.

(8) Vaughn, S. J.; Akhmatskaya, E. V.; Vincent, M. A.; Masters, A. J.; Hillier, I. H. *J. Chem. Phys.* **1999**, *110*, 4338.

(9) Ignaczak, A.; Gomes, J. A. N. F.; Cordeiro, M. N. D. S. *Electrochim. Acta* **1999**, *45*, 659.

(10) Xantheas, S. S. *J. Am. Chem. Soc.* **1995**, *117*, 10373.

(11) (a) Dang, L. X.; Garret, B. C. *J. Chem. Phys.* **1993**, *99*, 2972. (b) Gai, H.; Schenter, G. K.; Dang, L. X.; Garret, B. C. *J. Chem. Phys.* **1996**, *105*, 8835.

(12) (a) Markovich, G.; Pollac, S.; Giniger, R.; Cheshnovosky, O. *J. Chem. Phys.* **1994**, *101*, 9344. (b) Markovich, G.; Pollac, S.; Giniger, R.; Cheshnovosky, *Z. Phys. D: At. Mol. Clusters* **1993**, *26*, 98.

(13) (a) Robertson, W. H.; Diken, E. G.; Price, E. A.; Shin, J. W.; Johnson, M. A. *Science* **2003**, *299*, 1367. (b) Weber, J. M.; Kelley, J. A.; Nielson, S. B.; Ayotte, P.; Johnson, M. A. *Science* **2000**, *287*, 2461. (c) Weber, J. M.; Kelley, J. A.; Robertson, W. H.; Johnson, M. A. *J. Chem. Phys.* **2001**, *114*, 2698. (d) Myshakin, E. M.; Jordan, K. D.; Robertson, W. H.; Weddlle, G. H.; Johnson, M. A. *J. Chem. Phys.* **2003**, *118*, 4945. (e) Ayotte, P. G.; Weddle, H.; Kim, J.; Johnson, M. A. *J. Am. Chem. Soc.* **1998**, *120*, 12361.

(14) (a) Pathak, A. K.; Mukherjee, T.; Maity, D. K. *J. Chem. Phys.* **2006**, *125*, 074309. (b) Pathak, A. K.; Mukherjee, T.; Maity, D. K. *J. Chem. Phys.* **200**7, *126*, 034301. (c) Pathak, A. K.; Mukherjee, T.; Maity, D. K. *J. Chem. Phys.* **2007**, *127*, 044304.

(15) Price, E. A.; Hammeer, N. I.; Johnson, M. A. *J. Phys. Chem. A* **2004**, *108*, 3910.

(16) Pathak, A. K.; Mukherjee, T.; Maity, D. K. *J. Chem. Phys.* **2006**, *124*, 024322.

(17) Ramondo, F.; Sodeau, J. R.; Roddis, T. B.; Williams, N. A. *Phys. Chem. Chem. Phys.* **2000**, *2*, 2309.

(18) Engdahl, A.; Nelander, B. *J. Chem. Phys.* **1986**, *84*, 1981.

(19) Johnsson, K.; Engdahl, A.; Ouis, P.; Nelander, B. *J. Phys. Chem.* **1992**, *96*, 5778.

(20) (a) Mortia, A. *J. Comput. Chem.* **2002**, *23*, 1466. (b) Mortia, A.; Kato, S. *J. Chem. Phys.* **1999**, *110*, 11987.

(21) Jensen, L.; Swart, M.; van Duijnen, P. T.; Snijders, J. G. *J. Chem. Phys.* **2002**, *117*, 3316.

(22) Ghanty, T. K.; Ghosh, S. K. *J. Chem. Phys.* **2003**, *118*, 8547.

(23) Becke, A. D. *J. Chem. Phys.* **1993**, *98*, 1372.

(24) Schmidt, M. W.; Baldridge, K. K.; Boatz, J. A.; Elbert, S. T.; Gordon, M. S.; Jensen, J. H.; Koseki, S.; Matsunaga, N.; Nguyen, K. A.; Su, S. J.; Windus, T. L.; Dupuis, M.; Montgomery, J. A. *J. Comput. Chem.* **1993**, *14*, 1347.

(25) Schaftenaar, G.; Noordik, J. H. *J. Comp.-Aided Mol. Des.* **2000**, *14*, 123.

(26) Mayer, I. *Chem. Phys. Lett.* **198**, *97*, 270.

(27) (a) Sadlej, A. J. *Collect. Czech. Chem. Commun.* **1988**, *53*, 1995. (b) Sadlej, A. J.; Urban, M. *J. Mol. Struct.: THEOCHEM* **1991**, *234*, 147.